# scientific reports

Check for updates

OPEN

# A new insert drawing technique for controlling ore loss and dilution during sublevel caving

Xiaojing Meng, Tao Long, Xinyu Shi, Liyuan Wang, Zhonghua Zhu & Ganqiang Tao✉

Sublevel caving (SLC) is widely used in underground mines for its low cost and high production rate, but it faces challenges such as high ore loss and dilution. The previous research has focused on shape of draw bodies, stope structural parameters of SLC and drawing management. However, the flow of waste rocks, ore-rock contact and its control in the drawing process are not deeply studied. This study analyzed the main causes of these issues and the formation mechanism of waste rock funnels, proposing the insert drawing method (IDM) to reduce ore loss and dilution. This technique involves actively controlling the contact, movement direction, and path of ore-rock near the drawpoints using an insert device. By manipulating insert device, the technique effectively enhances ore flow velocity and area, resulting in enhanced ore recovery. By managing the movement of waste rock funnel, the technique can delay dilution entry in the drawpoints, effectively reducing ore dilution. Further, to validate IDM's effectiveness, comparative experiments were conducted between IDM and traditional cut-off grade drawing method (COGDM). The experimental results indicate that IDM outperforms COGDM in terms of ore recovery rate. For the mining of massive orebodies with SLC, IDM achieves a 10.96% higher ore recovery rate compared to COGDM; for steeply inclined medium-thick orebodies, IDM's ore recovery rate surpasses COGDM by 15.68–30.88%. The research demonstrates that IDM effectively reduces ore loss and dilution in SLC, making it suitable for widespread application in other SLC mines.

Sublevel caving method is widely used in underground mines across the world due to its safety, cost-effectiveness and high potential rate, etc.[1–3]. In China, more than 85% of underground iron ore mines and over 40% of non-ferrous metal mines utilize this method, accounting for about 25% of such mines globally. However, the SLC method faces significant challenges related to ore loss and dilution[4,5]. The average ore loss in SLC is 22%[6]. This issue is primarily attributed to the direct contact between blasted ores and overlying rocks during the drawing process[7]. The confined flow conditions, chaotic and random nature of material flow in SLC, and the impact of blasting extrusion make it difficult to control the ore-rock contact surface during extraction, leading to significant ore loss and dilution. Ore loss not only results in the wastage of mineral resources but also leads to substantial economic losses, while ore dilution can cause environmental pollution and damage. For example, in 2011, the production of iron ore resulted in 2.3 billion tons of waste rock and 636 million tons of tailings. The accumulation of tailings ponds and waste rock piles poses significant hazards, including risks of geological disasters such as dam breaks and debris flows. Tragic incidents like the collapse of a tailings pond in Xiangfen, Shanxi Province, China, in 2008, which led to 277 deaths and nearly $14 million in direct economic losses, underscore the seriousness of these risks. Addressing the ore loss rate of SLC by just 1% in China could potentially add 4 million tons of crude iron ore production annually. Therefore, reducing ore loss and dilution in SLC is not only crucial for resource conservation and economic efficiency but also for mitigating environmental impacts and preventing disasters.

To reduce ore loss and depletion in SLC, scholars both domestically and internationally have conducted extensive research including laboratory experiments, draw theories and full-scale tests[8,9]. Furthermore, numerous scholars have explored mining structures, structural parameters, and technological methodologies. Over 20 improvement strategies have been developed both globally and domestically, primarily focusing on adjusting SLC method parameters, with a few proposing modifications to the traditional scheme structures. For instance, Liang[10] introduced the concept of a wire rope-concrete flexible artificial roof and formulated a mechanical model based on soil arching theory. Malakhov[11] suggested the idea of ore fragment isolation, while

School of Resource and Environment and Safety Engineering, University of South China, Hengyang 421001, Hunan, China. ✉email: nhutgq@126.com

Chen[12] investigated the use of silicone rubber as a flexible isolation layer and analyzed the flow characteristics of caved ore within a single funnel. Cao and Ren introduced the diversion drawing technique to address dilution challenges in the extraction of inclined medium-thick orebodies, successfully implementing this technology at the Chambishi Copper Mine[13]. Subsequently, Tao[14] proposed an innovative diversion drawing technique. Recently, a novel mining method called lost-ore mining was introduced by Zhang, with successful applications observed at the Malmberget mine and the Kiruna mine[15]. Presently, more comprehensive theoretical frameworks include ellipsoid draw theory[11,16–18], random medium draw theory[19–21] and expectation body theory[22,23]. Although these studies have led to diverse improvements in the ore residual and waste mixing metrics associated with the SLC method, substantial breakthroughs have not been realized. Practical application has revealed that the findings of these studies have not produced significant outcomes, with ore loss and dilution in SLC remaining a significant challenge[7].

Over an extended period, previous research efforts have predominantly focused on aspects such as the shape of draw bodies, structural parameters of SLC, and draw management. However, there has been a notable lack of comprehensive research concerning the flow of waste rocks, as well as the formation and control of waste rock funnels during drawing process. Effective control of waste rock could potentially offer a fundamental solution to the challenges of ore loss and depletion. Therefore, the key to reducing loss and dilution in SLC lies in investigating the movement patterns of ore and rock, understanding the mechanisms behind loss and dilution, exploring methods to control the formation of waste rock funnels, and minimizing rock blending during the drawing process. To further reduce ore loss and depletion in SLC, this study proposes a novel drawing technique known as the insert drawing technique. This method aims to actively intervene in the interaction between ores and rocks, as well as the flow dynamics within the SLC method. For this purpose, we first conducted an analysis of the principle of the insert drawing technique. Then, a physical drawing model was designed and formulated based on a geometric similarity ratio of 1:50. Comparative experiments between traditional COGDM and IDM are then conducted, with the experimental results being analyzed and discussed. Finally, a thorough examination is undertaken to elucidate the reasons behind the efficacy of the insert drawing technique in reducing ore loss and depletion.

## Principle of the insert drawing technique
### The principle of the insert structure within silos

In industrial production, the flow of powdered materials within silos can lead to phenomena such as arching, segregation, and congestion during the discharge process. To improve the flow characteristics of powdered materials, various scholars have developed methods of using insert devices within silos. By incorporating insert structures, the objective is to enhance the flow trajectory and area of the powder within the silo, thereby increasing the flow rate of the powder[24–28].

The principle of the insert device is illustrated in Fig. 1. The silo comprises a vertical cylinder and a shrinking bin, both exhibiting axisymmetric shapes, with conical insert device symmetrically positioned within the silo. The central region of the bin represents a zone of rapid flow, where powder particles experience high and uniform flow rates. In contrast, surrounding this central area is the shear flow region, located in proximity to the silo's side walls. The introduction of conical inserts in the silo effectively enhances the flow rate of poorly flowing powders. Powder particles near the side walls experience accelerated flow rates, facilitating their discharge towards the bin outlet. Drawing inspiration from the principles of insert structures in silos, this paper introduces the concept of the insert drawing technique as a means to reduce the ore loss and depletion in SLC. The ore-drawing process involves the continuous release of ore-rock particles from drawpoints in production drifts, treating the caved ore-rock as individual particles.
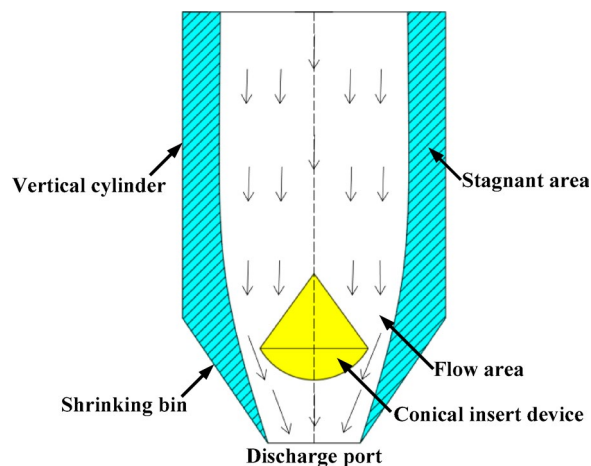


**Fig. 1**. The principle of the insert structure within silos.

## The principle of the insert drawing technique

The principle of the insert drawing technique is illustrated in Fig. 2. The primary concept behind the insert drawing technique involves altering the flow area of the blasted ores and caved rocks within the SLC stope through the utilization of an insert device[29]. The technology encompasses several key aspects. Initially, the insert device is positioned at the drawpoint within the drift, which serves as a critical location for ore-rock interaction. The insert structure comprises three insert plates oriented in the left, right, and upper directions. Subsequently, by manipulating the opening and closing sequence of the insert plates in various directions, control over the trajectory, direction, and velocity of the movement of the blasted ores and waste rocks can be achieved. Moreover, by adjusting the opening and closing sequence of the insert plates in different directions, the flow pattern and contact between the ores and rocks can be regulated, facilitating the effective segregation of waste rocks movement and thereby reducing ore loss and depletion. Through the strategic control of the waste rock funnel's movement, the technology can efficiently delay its rupture and the subsequent arrival at the drawpoint, effectively mitigating ore dilution. Further elucidation on the specific mechanisms underlying the reduction of ore loss and depletion will be discussed in more details in "Analysis of the mechanism of the insert drawing technique" section.

## Insert drawing sequence experiment
### Analysis of similitude

According to the similarity principle, when using laboratory physical simulation methods to analyze the drawing results of field experiments, it is essential to ensure geometric similarity, dynamic similarity, and kinematic similarity[30]. To meet dynamic similarity in the models, the similarity coefficient $\lambda_t$ must adhere to the following relationship: $\lambda_t = (\lambda_l)^{1/2}$, where $\lambda_l$ represents the length similarity coefficient. The mass similarity coefficient $\lambda_M$ is governed by the equation: $\lambda_M = m'/m$, ensuring dynamic similarity in the model. Here, m and m′ denote the mass within the stope and the mass in the model, respectively. Furthermore, the scale of the physical model holds significant importance in draw experiments. Trueman and Castro determined through experimentation on two distinct geometries that a 1:30 model scale outperforms a 1:100 scale[31,32]. In this study, a similar ratio of 1:50 was employed for experiment development.

## Experimental materials

In order to distinguish the ores and waste rocks in the experimental dispersion, dolomite is selected as the ore and black magnetite as the waste rock in the overlying strata. These materials are sourced from the mines. Given that the ore fragments are relatively large and unsuitable for direct utilization in physical simulation experiments, a small jaw crusher is employed to crush the ore into particles not exceeding 1 cm in size. By referencing the actual field grading, the particle size distribution of the crushed ores and waste rocks is determined. The cumulative size distribution curves for the different particle sizes are presented in Fig. 3. Following the determination of particle size distributions, the weighed particle materials are thoroughly mixed and stirred. The natural repose angle of the ore particles is measured to fall within the range of 30° to 33°.
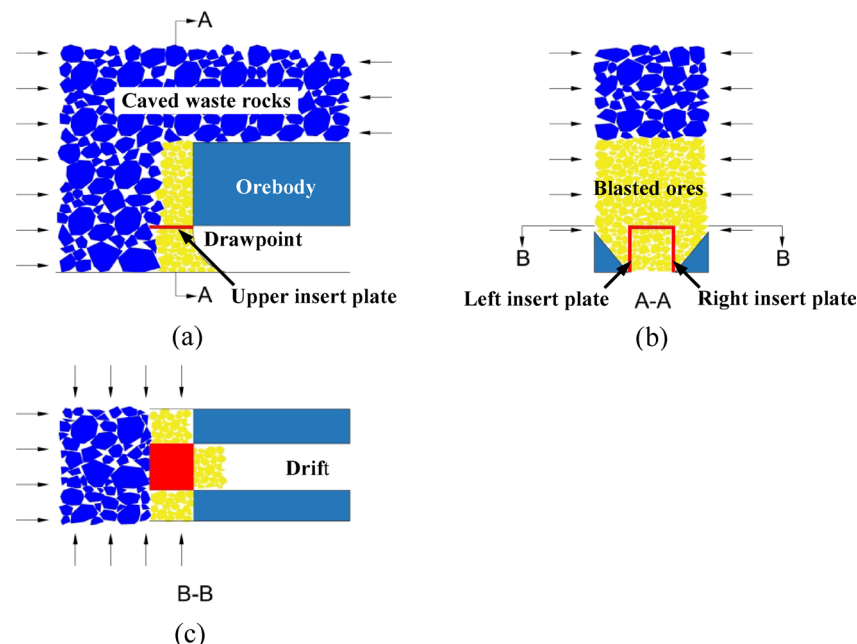


**Fig. 2.** Insert drawing stope structure diagram. (**a**) Transverse section of drift; (**b**) A–A Stope cross-section-al diagram; (**c**) B–B Top view.
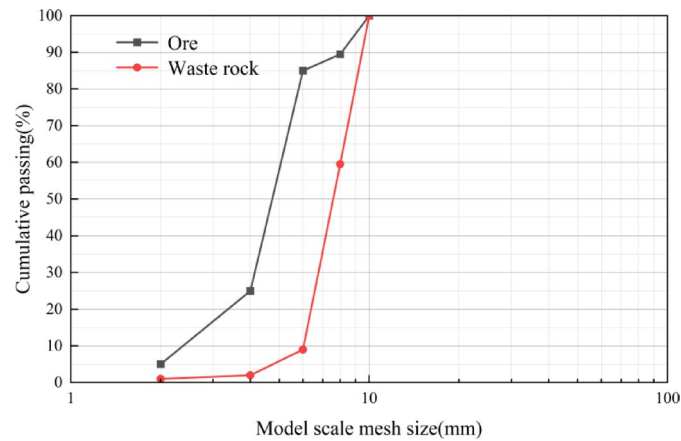
**Fig. 3**. Particle size distribution used in the insert drawing sequence experiment.

| Programs | Experiments | Total discharge/g | Total ore/g | Total waste rock volume/g | Waste rock blending rate/% | Ore recovery rate/% |
|---|---|---|---|---|---|---|
| Right-upper-left | Exp 1 | 13,504 | 7336 | 6169 | 45.68 | 56.84 |
| | Exp 2 | 13,165 | 7308 | 5857 | 44.49 | 56.62 |
| | Average value | 13,335 | 7322 | 6013 | 45.09 | 56.73 |
| Upper-right-left | Exp 1 | 13,507 | 7154 | 6353 | 47.03 | 55.42 |
| | Exp 2 | 13,227 | 7113 | 6114 | 46.23 | 55.11 |
| | Average value | 13,367 | 7133 | 6234 | 46.63 | 55.26 |
| Right-left-upper | Exp 1 | 13,184 | 7684 | 5500 | 41.71 | 59.53 |
| | Exp 2 | 12,667 | 7569 | 5098 | 40.25 | 58.64 |
| | Average value | 12,925 | 7627 | 5299 | 40.98 | 59.09 |

**Table 1**. Experimental results of the opening sequences of the insert plates.

## Experimental model and scheme

To achieve the optimal drawing effect of IDM, an experimental investigation on the drawing sequence of IDM was conducted. A model with a similarity ratio of 1:50 was devised for this purpose. The model is segmented into two sublevels, with particles in each sublevel loaded sequentially from top to bottom as waste rock overburden and ore, respectively. Each sublevel comprises 5 ring burdens. The model features a sublevel height of 10 m, a ring burden of 2 m, and a drift width and height of 3 m each. Constructed from transparent acrylic boards, the model includes an insert structure composed of three closely positioned insert plates adjacent to the drift wall, as depicted in Fig. 2. In order to replicate blasting effects, burden plates were interspersed between each ring within the model. Both the burden plates and insert plates are crafted from 1 mm thick steel plate material. The experiment was designed to vary the opening sequence of the insert plates, resulting in three distinct experimental schemes and a total of six groups. The specific details of the experimental scheme are outlined in Table 1, guiding the execution of the experiments to explore the most effective draw sequence for IDM operations.

## Experimental processes

The loading process of the experimental model is illustrated in Fig. 4. Initially, the burden plate was inserted into the slot, followed by filling the model with dolomite, the ore material. To ensure a uniform distribution of ores within each burden, precise weighing of the dolomite mass at each ring burden was crucial, allowing for the accurate calculation of the total mass during the loading process. Subsequently, after filling the model with ores, the upper sublevel was filled with iron ores, representing the waste rock. In this experimental setup, the cut-off control method was used to end drawing in the experiments. This method dictates that when the volume ratio of waste rock to ore in a single drawing step reaches 3:1, it signifies the cessation of drawing from the drawpoint.

The IDM process is delineated as follows. In accordance with the experimental design outlined earlier, distinct experiments were carried out, with the opening sequence of the insert plates specified as "Right-Upper-Left" for illustration purposes. Initially, the ores were drawn out by opening the right insert plate, and drawing operations ceased upon reaching the cut-off grade condition. Subsequently, the right insert plate was reinstated to its original position. Secondly, the upper insert plate was opened to extract the ore and rock materials from the drawpoint, halting draw activities once the discharged loose material met the cut-off grade. These procedures were repeated until the ore extraction on the left side was finalized. Upon completion of ore extraction at the current burden, the subsequent ring was detonated. This iterative process continues until the entire sublevel drawing is accomplished. Following the conclusion of drawing operations for this sublevel, the drawing of the subsequent sublevel commences, following the same procedures as those employed for the upper sublevel.
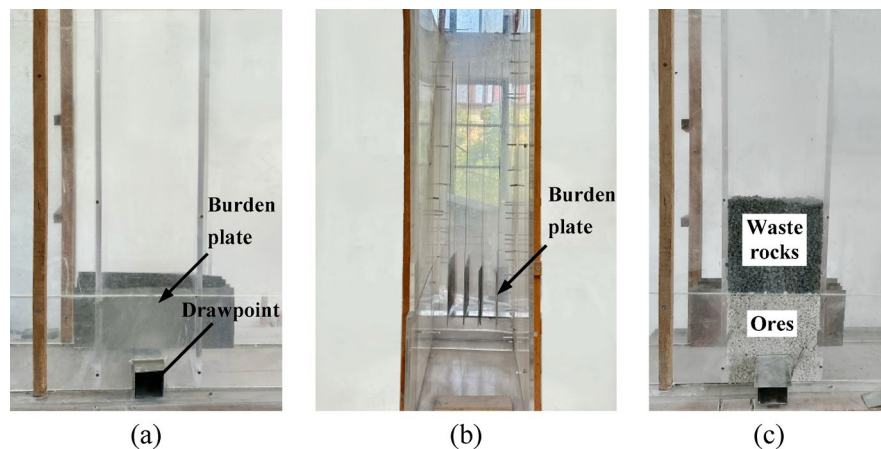
**Fig. 4**. Experimental model diagram for insert drawing. (**a**) Model front view; (**b**) Model side view; (**c**) Loading model front view.

### Analysis of experimental results

The results of the opening sequence-dependent IDM experiments are presented in Table 1. Based on the data displayed in the chart and table, the average ore recovery rates for the three mining schemes were 56.73%, 55.26%, and 59.09%, respectively, while the average waste rock blending rates were 45.09%, 46.63%, and 40.98%, respectively. In comparison to the other two schemes, the experimental outcomes associated with the opening sequence of "Right-Left-Upper" exhibited the highest ore recovery and the lowest dilution, representing the most favorable experimental results. Consequently, the mining sequence involving the insert drawing structure will be adopted for the forthcoming experiments.

## Comparative experiments between COGDM and IDM for the mining of massive orebodies

### Experimental model and protocol

Following the determination of the optimal opening sequence for IDM, a comparative experiment was conducted to validate the feasibility of IDM. The experiment used a self-designed physical drawing model with a geometric scale of 1:50. The size of the model was $0.8 \times 0.22 \times 1.1$ m$^3$ (length $\times$ width $\times$ height). Transparent acrylic glass panels, 10 mm in thickness, were installed around the model to enhance the visibility of ore and rock flow dynamics during the drawing process. The model was segmented into 5 sublevels, each with a sublevel height and drift spacing of 10 m. Within each sublevel, 5 drawing steps were established, with a 2 m spacing between each step. The size of drift is $3 \times 3$ m$^2$ (width $\times$ height). The insert plates and burden plates were constructed from 1 mm thick steel plates. Five longitudinal slots measuring 1.5 mm in width are precisely machined on the acrylic side panels of the model, extending vertically from the top of the current sublevel drawpoint to the bottom of the upper sublevel drawpoint. During model assembly, the burden plates are inserted through these slots from one side of the model to the opposite side.

The experimental model is shown in Fig. 5, where the top sublevel represents the waste rock cover layer, while the lower four sublevels signify ore layers. The experiment entailed two distinct drawing schemes: the IDM experiment and the COGDM experiment. Each experiment was replicated twice, resulting in a total of four experimental groups. The bulk materials and gradations utilized in this experiment mirrored those outlined in "Insert drawing sequence experiment" section. The experimental procedures closely resembled those detailed in "Insert drawing sequence experiment" section; hence, this section does not delve into specific process details.

### Comparison results of two types of drawing methods

The experimental results of COGDM and IDM were shown in Table 2. Based on the specific experimental data, the average ore recovery rate and waste rock blending rate for COGDM were 72.21% and 50.1%, respectively. For IDM, the average ore recovery rate and waste rock blending rate were 83.17% and 55.67%, respectively. From experimental results, it was observed that the ore recovery rate of IDM was higher than that of COGDM by 10.96%.

### Analysis of ore loss and dilution in each sublevel

The detailed information regarding ore residual and waste mixing for each sublevel under the two drawing methods is presented in Table 2, accompanied by visual representations in Fig. 6. As indicated in Table 2, in the first to fourth sublevel, IDM outperformed COGDM by 36.26%, 0.46%, 3.63%, and 3.48% in the four sublevels. There was a significant disparity in ore recovery rates between the two in the first sublevel, while the differences were minimal in the other three segments. Particularly in the third sublevel, there was a notable increase in ore recovery rates. The diamond-shaped stope structure and increased number of production drifts in the third sublevel enhanced ore recovery by efficiently extracting residual ores between the drifts in the upper sublevel.
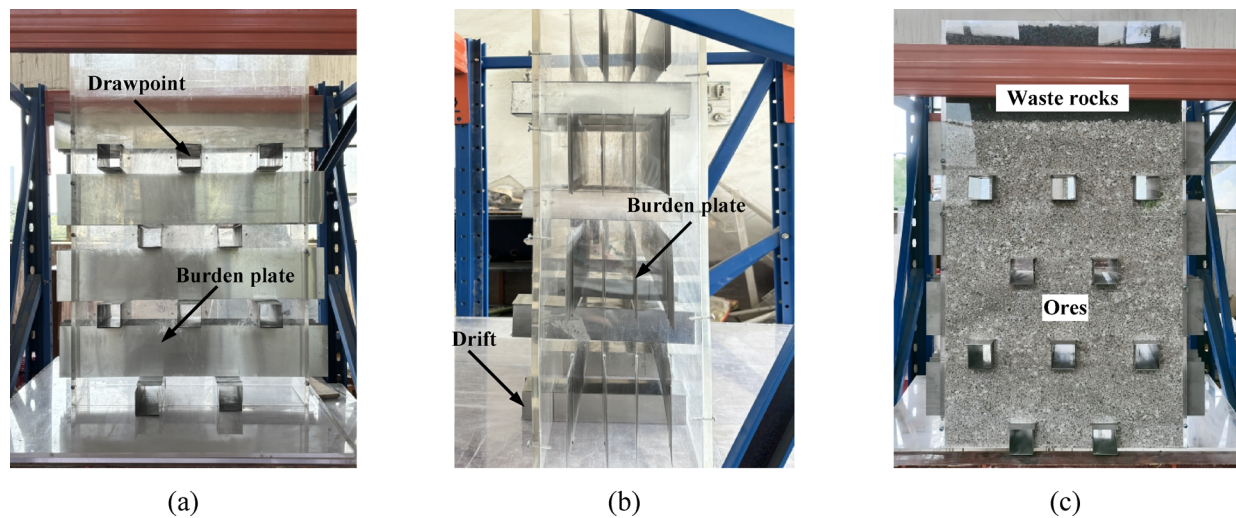
(a)　　　　　　　　　　　　　(b)　　　　　　　　　　　　　(c)

**Fig. 5**. Experimental loading model diagram between IDM and COGDM. (**a**) Model front view; (**b**) Model side view; (**c**) Loading model front view.

| Drawing method | Experiments | Drawing indices | SL 1 | SL 2 | SL 3 | SL 4 | Total |
|---|---|---|---|---|---|---|---|
| COGDM | Exp 1 | Ore recovery rate/% | 33.95 | 66.95 | 129.13 | 64.87 | 70.70 |
| | | Waste rock blending rate/% | 58.23 | 47.45 | 52.43 | 46.92 | 49.15 |
| | Exp 2 | Ore recovery rate/% | 32.28 | 67.63 | 116.22 | 66.66 | 73.72 |
| | | Waste rock blending rate/% | 52.78 | 45.56 | 51.43 | 46.34 | 51.04 |
| | Average value | Ore recovery rate/% | 33.11 | 67.29 | 122.67 | 65.76 | 72.21 |
| | | Waste rock blending rate/% | 55.51 | 46.50 | 51.93 | 46.63 | 50.1 |
| IDM | Exp 1 | Ore recovery rate/% | 67.03 | 68.13 | 125.99 | 69.44 | 82.65 |
| | | Waste rock blending rate/% | 58.48 | 55.95 | 53.46 | 55.51 | 55.50 |
| | Exp 2 | Ore recovery rate/% | 71.71 | 67.37 | 126.62 | 69.05 | 83.69 |
| | | Waste rock blending rate/% | 57.62 | 55.46 | 55.15 | 55.54 | 55.84 |
| | Average value | Ore recovery rate/% | 69.37 | 67.75 | 126.30 | 69.24 | 83.17 |
| | | Waste rock blending rate/% | 58.05 | 55.71 | 54.31 | 55.52 | 55.67 |

**Table 2**. Comparison of drawing indices for each sublevel (SL) between IDM and COGDM.

From the first to the fourth sublevel, IDM showed waste rock blending rates that were 2.54%, 9.21%, 2.38%, and 8.89% higher than COGDM, respectively. In the first and third sublevels, the differences in waste rock blending rates between the two were not significant; however, in the second and fourth sublevels, there were substantial differences. There are two main reasons for the high dilution in IDM. One is a reduction in the number of drifts compared to the previous sublevel. Second, the ore recovery rate can be improved to a certain extent by increasing the dilution rate.

IDM consistently outperformed COGDM, maintaining a 10.96% higher cumulative ore recovery rate across all sublevels. This indicates a significant overall ore recovery advantage for IDM. Conversely, IDM's waste rock blending rate was 5.57% higher than COGDM's, but the disparity was not substantial. In conclusion, IDM showcases superior ore recovery capabilities compared to COGDM.

## Comparative experiments between COGDM and IDM for the mining of steeply inclined medium-thick orebodies
### Experimental model and protocol

Based on the similitude principle, a scaled physical model with a geometrical scale of 1:50 was designed for drawing, as shown in Fig. 7. The model, constructed from 10 mm thick acrylic glass, allowed for the observation of particle flow dynamics during drawing. Wooden strips were strategically positioned around the model to bolster stability. The model was segmented into three sublevels: the upper sublevel represented the overlying waste rock, while the two lower sublevels depicted the orebody. Five rings were designed and the burden between blast rings was in the order of 2 m. The drift (the width and height were both 3 m) were located on the bottom of the footwall and were made of steel plates.

To account for variations in ore body characteristics, 12 distinct experimental schemes were devised, encompassing orebody dip angles spanning from 60° to 85° and orebody widths ranging from 6 to 10 m.
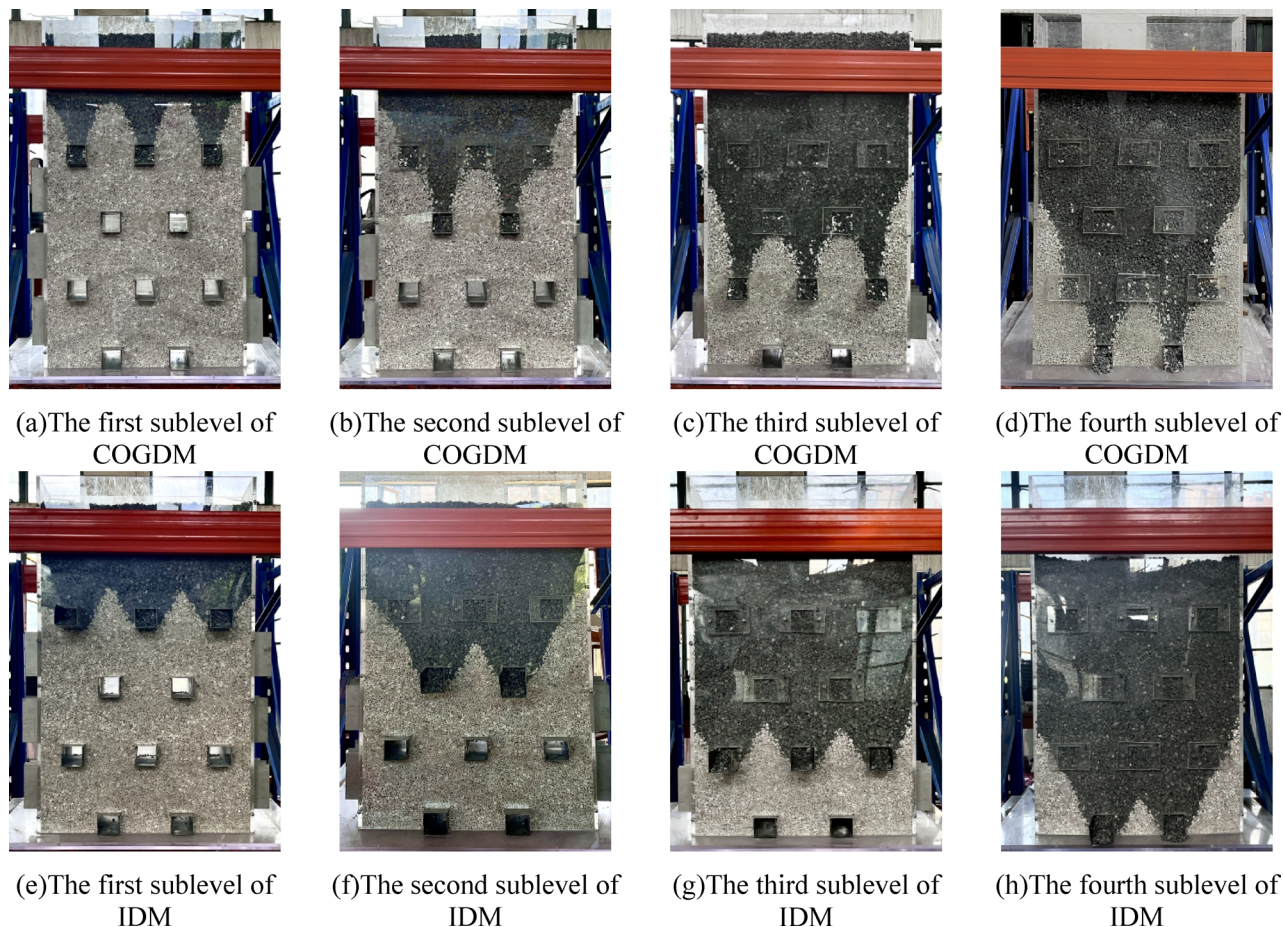
(a)The first sublevel of COGDM

(b)The second sublevel of COGDM

(c)The third sublevel of COGDM

(d)The fourth sublevel of COGDM

(e)The first sublevel of IDM

(f)The second sublevel of IDM

(g)The third sublevel of IDM

(h)The fourth sublevel of IDM

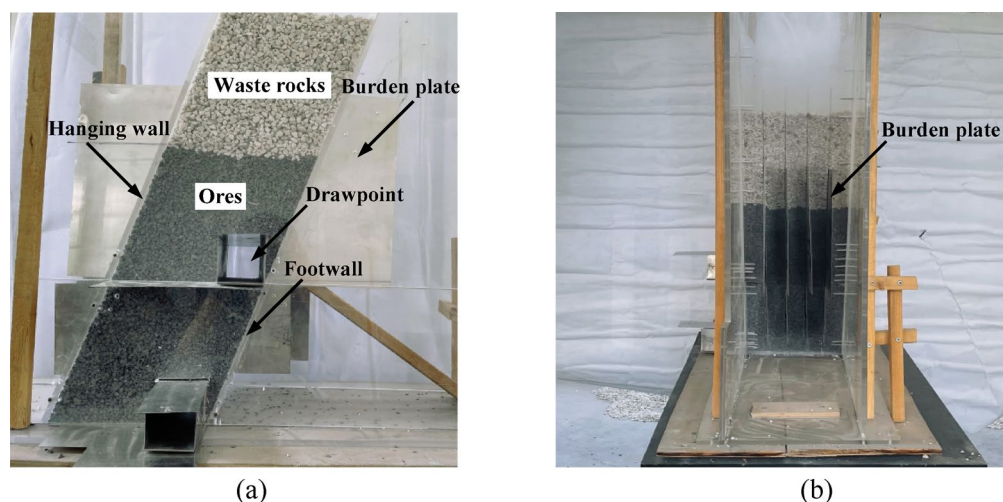**Fig. 6**. Partial results of the comparative experiment between IDM and COGDM.



(a)

(b)

**Fig. 7**. Experimental loading model diagram. (**a**) Loading model front view; (**b**) Loading model side view.

Following each set of IDM experiments, a corresponding set of COGDM comparative experiments was undertaken, resulting in a total of 24 experiment groups. The specific experimental schemes were detailed in Table 3. Magnetite and dolomite were used as the simulation materials in the experiments, in which magnetite was regarded as blasted ore and dolomite was deemed as overlying waste rock. The experimental gradation aligned with the methodology employed in "Insert drawing sequence experiment" section, and the experimental

| Program | Orebody dip angle/° | Orebody width/m | Waste rock blending rate/% | | | Ore recovery rate/% | | |
|---|---|---|---|---|---|---|---|---|
| | | | COGDM | IDM | Increase value | COGDM | IDM | Increase value |
| 1 | 60 | 10 | 43.42 | 30.97 | − 12.45 | 46.63 | 69.09 | 22.46 |
| 2 | 65 | 10 | 36.67 | 37.63 | 0.96 | 47.40 | 70.39 | 22.99 |
| 3 | 70 | 10 | 36.94 | 38.38 | 1.44 | 52.18 | 74.03 | 21.85 |
| 4 | 75 | 10 | 44.05 | 46.50 | 2.45 | 54.83 | 75.74 | 20.91 |
| 5 | 80 | 10 | 41.27 | 45.21 | 3.94 | 56.90 | 76.95 | 20.05 |
| 6 | 85 | 10 | 41.45 | 44.73 | 3.28 | 59.03 | 77.35 | 18.32 |
| 7 | 60 | 6 | 40.21 | 52.34 | 12.13 | 49.83 | 70.87 | 21.04 |
| 8 | 65 | 6 | 36.98 | 44.65 | 7.67 | 50.14 | 76.12 | 25.98 |
| 9 | 70 | 6 | 34.21 | 38.93 | 4.72 | 56.73 | 79.91 | 23.18 |
| 10 | 60 | 8 | 40.43 | 46.93 | 6.5 | 46.73 | 70.01 | 23.28 |
| 11 | 65 | 8 | 33.40 | 45.85 | 12.45 | 47.71 | 73.11 | 25.40 |
| 12 | 70 | 8 | 37.93 | 42.25 | 4.32 | 55.70 | 74.95 | 19.25 |

**Table 3**. Comparison experimental results between COGDM and IDM (sublevel height is 10 m).

process mirrored that of the experiment in "Comparative experiments between COGDM and IDM for the mining of massive orebodies" section.

### Comparison results of two types of drawing methods

The experimental results presented in Table 3 demonstrate that the ore recovery rate of IDM surpasses that of the conventional COGDM when mining orebodies of varying thicknesses and dip angles. Specifically, in the extraction of the steeply inclined medium-thick orebodies (with width ranging from 6 to 10 m and dip angles from 60° to 85°), IDM achieved ore recovery rates between 69.09 and 79.91%, which was higher than conventional COGDM 18.32–25.98% and the average increase was 22.06%. The waste rock blending rate ranged from 30.97 to 52.34%, with IDM demonstrating an average reduction of 3.95% compared to COGDM. The notable improvements in ore recovery rates and waste rock blending rate highlight the effectiveness of IDM compared to traditional COGDM methodologies in this specific mining context.

## Analysis of the mechanism of the insert drawing technique
### The formation mechanism of waste rock funnel

In SLC method, mining operations progress sequentially from top to bottom, with ore blasted out in a fan pattern from the sublevel drifts, causing the overlying rock mass to cave spontaneously under the influence of gravity. The blasted ores and caved waste rocks form a gravity flow as blasted ore is loaded from the sublevel drifts, with the waste rock content increasing gradually as extraction proceeds, leading to a dilution of the metal grade. Therefore, the primary objective in SLC is to achieve reasonable ore recovery while maintaining the dilution rate within an acceptable range[33].

Studies have shown that the geometry of the width of draw body or isolated extraction zone (IEZ) increases with the height of IEZ. This means that as the extraction zone becomes taller, the width of the area where ore is being drawn out also increases. This widening of draw body or IEZ is an important consideration in SLC method as it impacts the efficiency of ore extraction and the management of waste rock.

As shown in Fig. 8, a waste rock funnel above the drawpoint gradually forms at the interface between the ore and rock, descending towards the drawpoint. When the draw body is situated within the blasted ore layer, the waste rock funnel has not yet reached the drawpoint, allowing for the extraction of pure ore. At the point where the IEZ reaches the ore-rock contact surface, the lowest point of the waste rock funnel coincides with the drawpoint, facilitating the maximum extraction of pure ore.

Continuing the loading process leads to the release of the waste rock funnel tip, transforming it into a broken funnel where waste rocks mix with the ores, resulting in a blended material of ore and rock. Subsequent drawing operations cause the cross-sectional area of the broken funnel mouth to progressively expand, increasing the proportion of waste rock released. Consequently, the grade of the extracted ore diminishes continuously until the cut-off grade is attained, signaling the cessation of loading from the drawpoint.

Based on the preceding analysis, it can be seen that the rupture of the waste rock funnel at the apex of the drawpoint is one of the important reasons for ore depletion during the drawing process. Furthermore, two significant factors leading to dilution during ore extraction are identified. Illustrated in Fig. 9, at the front of the drawpoint, as loading progresses, the draw body expands continuously, along with a corresponding increase in its width. Upon the draw body encountering waste rocks from previous blasted rings in front, the rupture of the waste rock funnel at the drawpoint's forefront occurs, resulting in ore dilution. Simultaneously, when the draw body interacts with waste rocks on the upper left and upper right sides of the drawpoint, the waste rock funnels surrounding the drawpoint also rupture, causing dilution. The aforementioned observations underscore that the rupture of the waste rock funnel at the drawpoint from four directions (upper, front, left and right) plays a pivotal role in the ore dilution observed in the SLC drawing process. This is also the formation mechanism of waste rock funnel and the main cause of ore dilution in SLC drawing process.
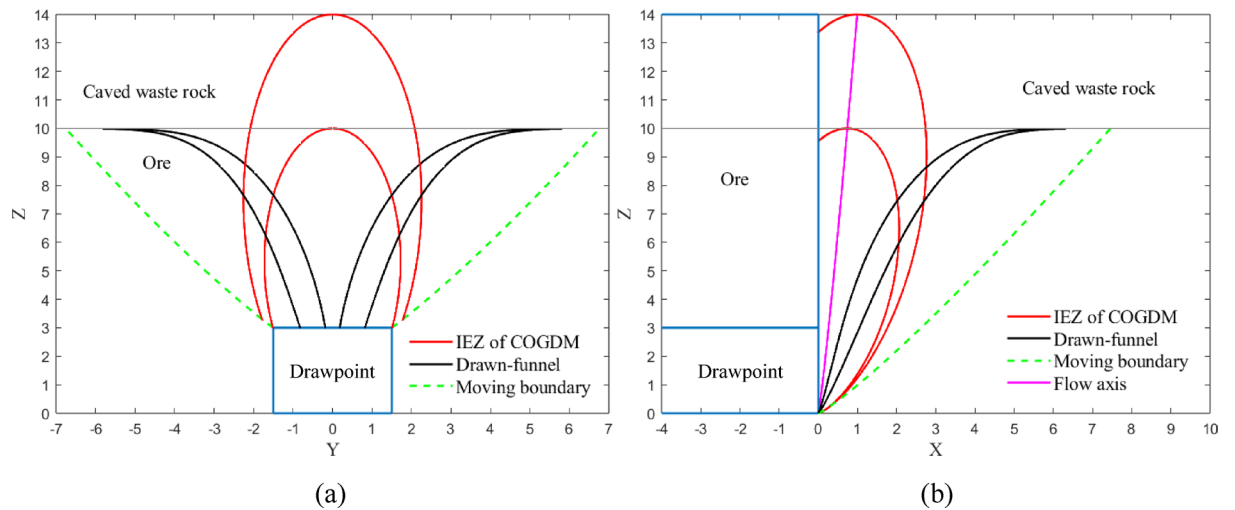
**Fig. 8**. The IEZ and waste rock funnel in the drawing progress of SLC. (**a**) Longitudinal section of drift; (**b**) Transverse section of drift.
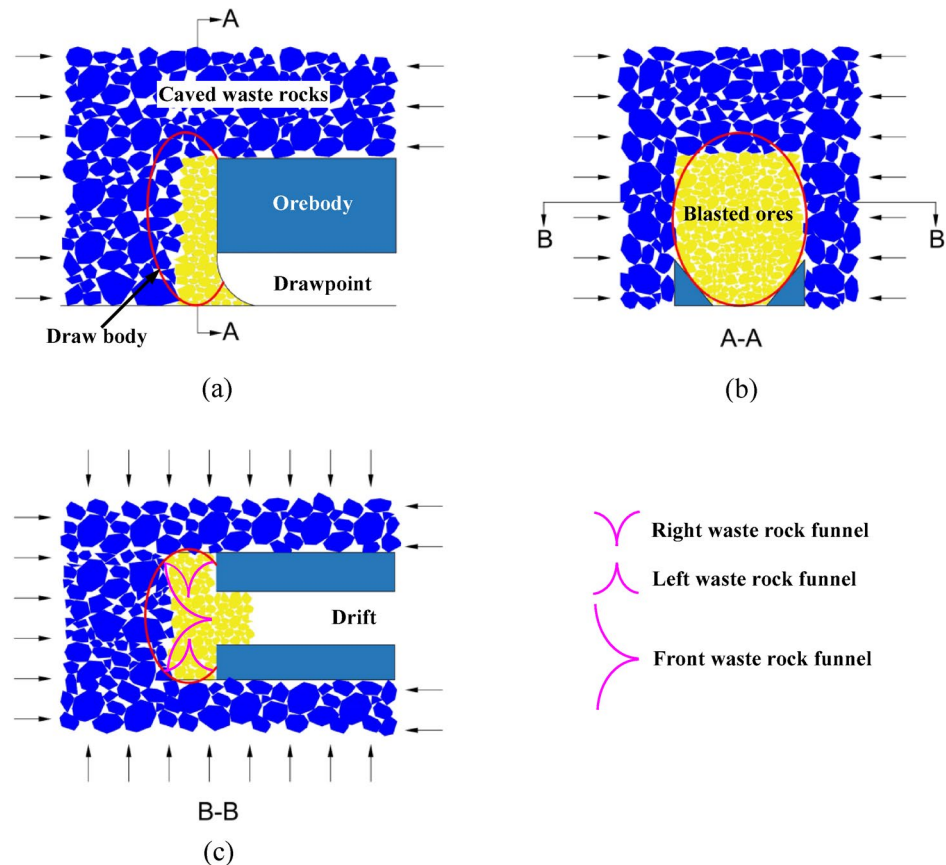


**Fig. 9**. Waste rock funnels and draw body diagram. (**a**) Transverse section of drift; (**b**) Longitudinal section of drift; (**c**) Top view.

The main reason for waste rock funnel fracture is the mismatch between the stope structure parameters and the shape of the draw body. If the sublevel height is insufficient, the waste rock funnel above the drawpoint may fracture during extraction. And an excessive drawing step can lead to the breakage of the waste rock funnel in front of the drawpoint. Inadequate spacing between drifts can result in the fracture of waste rock funnels on both sides of the drawpoint during extraction. The sequence in which these four waste rock funnels manifest may vary, as well as the time taken to reach the drawpoint. This phenomenon is associated with the stope structure

parameters of SLC and draw management practices, etc. Furthermore, the main cause of ore dilution in SLC is the blending of ores and rocks during the ore blasting and ore-rock flow process.

## The main causes of ore loss

Several factors influence ore recovery in SLC, including SLC designs, drill and blast design, seismic events and rock bursts, grade control, geological considerations, as well as factors like rock drilling and rock support. In addition to these factors, ore residual and waste mixing in SLC method are influenced by factors such as overburden rock characteristics, shovel depth, and drawing management practices, etc. In addition, key factors influencing ore recovery performance include sublevel height, drawpoint size, and ore-rock particle size distribution in the sublevel caving method. These factors interact with geological conditions such as ore body dip and thickness. Therefore, optimizing ore drawing performance requires comprehensive consideration of matching stope structural parameters with flow properties of broken ore-rock masses.

When ore extraction from a SLC ring is completed, there are often some blasted ores that are left in the waste rocks at and above the drawpoint. These remained ores are termed residual ores and encompass four categories: ridge ore remnants between sublevels, frontal ore remnants following each drawing step, wall-adhering ore remnants situated near the vertical ore mass wall, and foot-wall ore remnants within the inclined ore body[34]. The positions of these ore remnants are illustrated in the yellow ores in Fig. 10.

The formation of ridge ore remnants stems from the ongoing development of the IEZ, causing a substantial influx of waste rocks from above and in front to swiftly flow towards the drawpoint. Ores situated on either side of the drift moves at a slower pace. Upon reaching the cut-off grade during ore extraction, a portion of the ores on both sides remains unextracted. Furthermore, due to the spacing between adjacent drifts, some ores persist between neighboring production drifts, giving rise to ridge remnants. Given the rhombic layout of the production drifts, the ridge remnants from upper drifts can be partially recovered in lower drifts.

The presence of wall-adhering ore remnants is primarily attributed to the influence of the end wall on the IEZ during the extraction process, causing the flow axis to deviate from perpendicular alignment with the central axis of the production drift. Following the extraction of pure ores, waste rocks from the overlying strata and previous steps swiftly flow towards the drawpoint, hastening the attainment of the cut-off grade in this stage of ore extraction and resulting in an increased presence of wall-adhering remnants.

The presence of frontal ore remnants can be attributed to the cessation of drawing at each extraction step, resulting in the generation of residual material. This occurs because, following the extraction of the majority of pure ores, the waste rocks located at the top and front of the step swiftly intermixes and is extracted. The remaining undrawn ores, along with some remnants adhering to the walls from the preceding draw step, contribute to the formation of frontal remnants. Additionally, inadequate shoveling depth during ore extraction leads to the accumulation of frontal remnant ores within the production drifts, obstructed by external waste rocks. Frontal remnants are typically partially recovered in lower drifts.

The remnant ores move downward and interact with waste rocks, leading to the formation of an ore-rock mixed layer. If the grade of this mixed layer surpasses the cut-off grade, it retains value for utilization. During ore extraction in the lower sublevel, remnant ores, particularly ridge and frontal remnants, can descend towards drawpoints, allowing for potential re-extraction. However, other blasted ores that cannot be released will become a permanent ore loss. Consequently, ore loss can be categorized into ridge lost ores, foot-wall lost ores, wall-adhering lost ores, and frontal lost ores. The possibility of extraction depends primarily on the economic worth of the ore-rock mixed layer and its ability to reach the drawpoints situated within the production drifts.

## Analysis of the reasons for insert drawing technique to reduce ore loss and dilution

Based on the previous analysis, it is evident that the extent of ore dilution and loss can be managed by restricting the advancement of the IEZ, specifically by limiting the degree of fracturing in the waste rock funnels. The subsequent discussion delves into the mechanism of reducing ore residual and waste mixing in the insert drawing technique by focusing on controlling the IEZ and waste rock funnels.
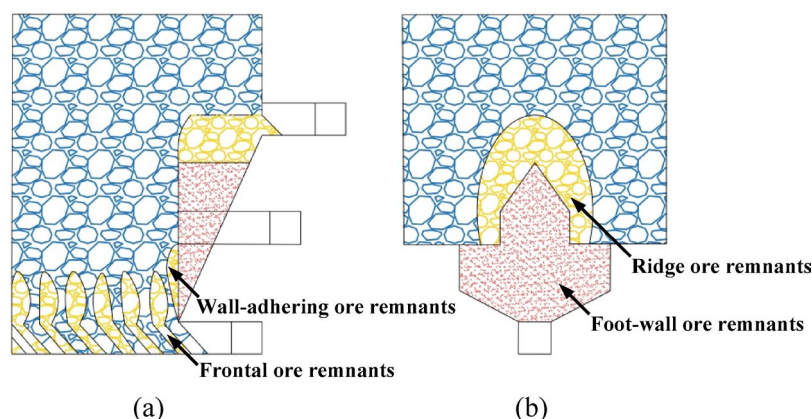


**Fig. 10**. Ore remnants positions. (**a**) Transverse section of drift; (**b**) Longitudinal section of drift.

Referring to a previous drawing experiment where the sublevel height was 10 m and the drift dimensions were $3 \times 3$ m², in conventional drawing, the evolution of the draw body is depicted in Fig. 11a. In Fig. 11a, the purple IEZ symbolizes the extraction of pure ores. As the drawing process continues, the IEZ will transition into the ore-rock contact layer. When the IEZ reaches a height of 14 m, the red draw body contains some waste rocks and concurrently releases a greater amount of ores compared to the purple draw body. When the draw height reaches a certain value, such as 14 m, the loading is stopped because the grade of extracted granular material reaches the cut-off grade. It becomes apparent from Fig. 11a that a substantial quantity of ore remains in this sublevel. These remnants constitute the primary source of residual ores in the ridge.

When employing the insert drawing technique, the right insert plate was initially activated. The progression of the IEZ is illustrated in Fig. 11b. At a draw height of 14 m, the blue IEZ liberates a greater quantity of ores compared to the red IEZ, as denoted by the ABCD region in Fig. 11b, indicating a concurrent reduction in residual ores within the ridge. Furthermore, ore extraction from the upper right section of drawpoint implies a decline in residual ores adhering to the wall and frontal residual ores during subsequent mining operations. Upon opening the left insert plate, the evolution of the IEZ is delineated in Fig. 11c. Similarly, in comparison to the conventional drawing method, there is a discernible decrease in the residual ores within the ridge, residual ores attached to the wall, and frontal residual ores to varying extents. Additionally, upon opening the upper insert plate, a significant portion of the ore situated above the drawpoint can be reclaimed, leading to varied reductions in residual ores attached to the wall and frontal residual ores during this phase. As depicted in Fig. 11d, the red area is the ore range that can be extracted by COGDM in the plane. The range of ores produced by IDM includes blue areas as well as red areas. It can be seen that IDM signally increases the mining area of ore compared with COGDM.

Drawing from the principles of random medium draw theory, the velocities and trajectories of waste rock particles in the XZ and YZ planes at $Z = 10$ m are delineated in Fig. 12. Three representative waste rock particles at the ore-rock interface, denoted as points A, B, and C, are selected for elucidation. In Fig. 12a, it is evident
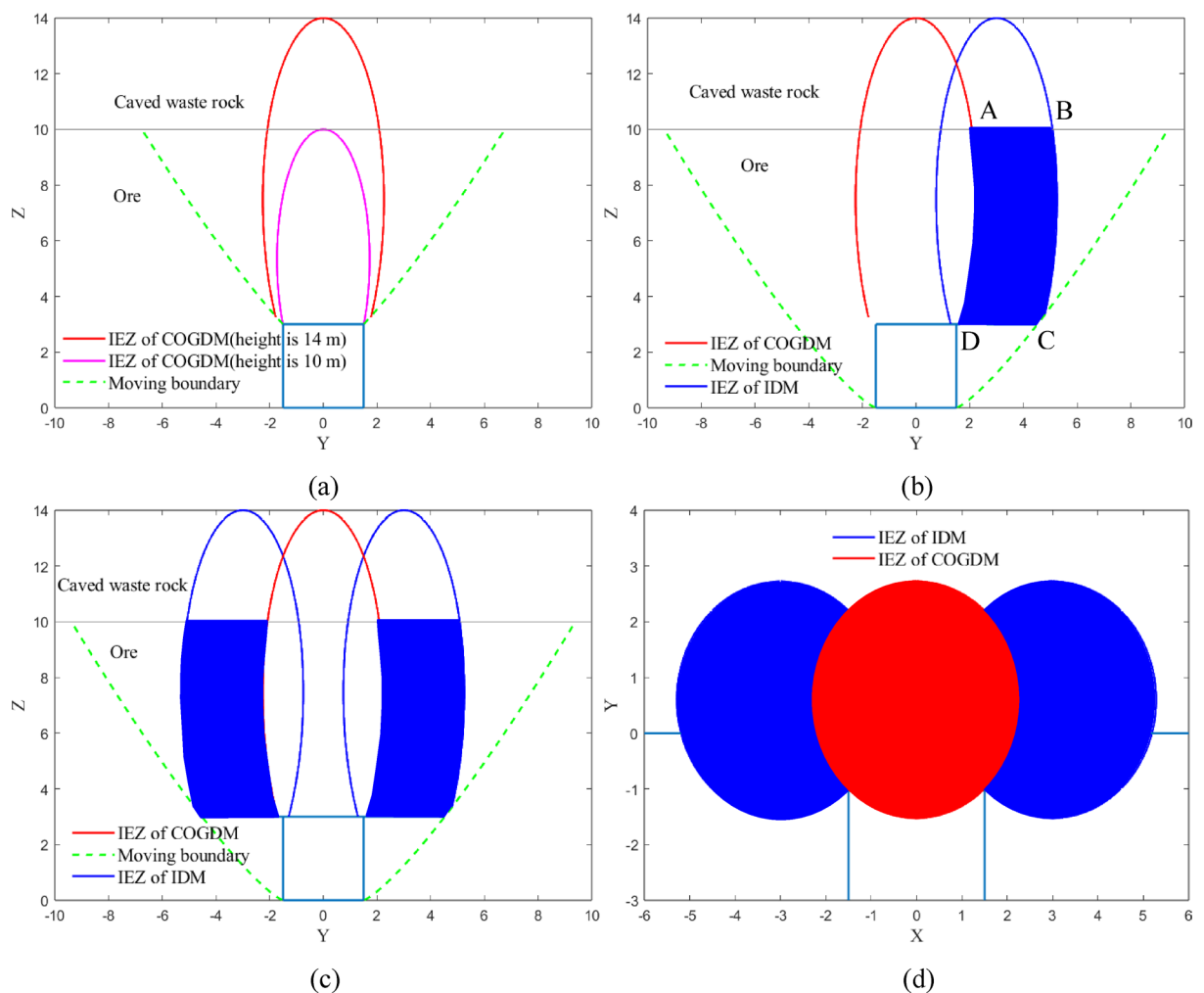


**Fig. 11.** The IEZ in the drawing progress of SLC. (**a**) IEZ for COGDM; (**b**) IEZ for IDM (opening the right insert plate); (**c**) IEZ for IDM (opening the left insert plate); (**d**) Comparison of IEZ between COGDM and IDM from top view.
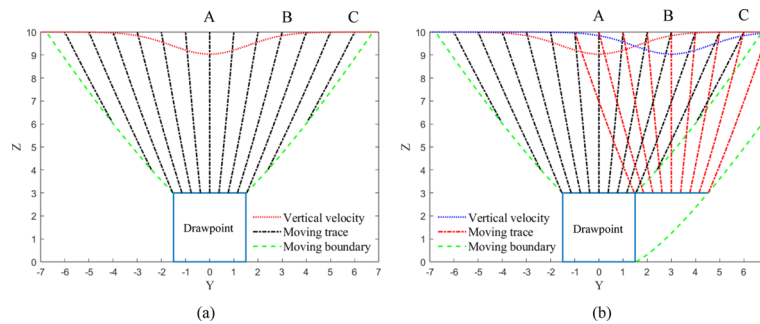
**Fig. 12**. Comparison diagram of vertical velocity and moving trace between IDM and COGDM. (**a**) Transverse section of drift of COGDM; (**b**) Transverse section of drift of IDM.

that during conventional COGDM, the flow velocity is highest at point A (0, 0, 10), followed by point B (0, 3, 10), while the flow velocity at point C (0, 6, 10) approaches zero. Analysis of the particle trajectories reveals that waste rock particles at point A swiftly converge towards the drawpoint along the flow axis, leading to ore dilution. Conversely, in the IDM, the presence of the insert structure imposes constraints on the movement and fracturing extent of the waste rock funnel, thereby facilitating control over the degree of ore dilution.

In Fig. 12b, the impact of IDM on the flow velocities and paths of waste rock particles at points A, B, and C along the ore-rock interface is evident. Notably, there are notable alterations in the flow characteristics. The flow velocity at point B emerges as the highest, while the velocities at points A and C are approximately equivalent. The reduced flow velocity and elongated trajectory at point A suggest a deceleration in the downward movement trend of waste rock funnel in the vicinity of point A. Conversely, the escalated flow velocities and shortened trajectories at points B and C indicate that the initially sluggish-moving ores situated above the drawpoint on the right side can experience enhanced downward movement speed and expanded flow area due to the presence of the insert structure. This phenomenon stands as a key factor contributing to the heightened ore recovery rate. Upon opening the left-side insert plate, further control over the movement and fracturing extent of the waste rock funnel, as well as the ore recovery rate, can be achieved. The underlying principle mirrors that described above and hence does not necessitate further elaboration. At the same time, the control principle of the three waste rock funnels in other directions (front, left and right sides) of the drawpoint is similar, so it will not be discussed in detail.

## Discussions

There are many factors that influence the ore recovery efficiency in mining operations, such as size of drawpoint, size and distribution of ore rock particles, orebody dip, orebody thickness, sublevel height, extraction drift spacing, ring burden, etc.[35] This paper conducted a comparative experiment between COGDM and IDM, revealing the new technology's advantageous role in reducing ore residual and waste mixing within the SLC method. The research only focuses on the effects of orebody dip and thickness. Furthermore, since the study of the insert drawing technique is only carried out in the laboratory, the contact and movement of ore-rock in the experiment are easily controlled. Laboratory findings may not perfectly align with field trial results, underscoring the necessity for further field experiments to authenticate real-world mining outcomes.

Potential enhancements to enhance ore recovery in IDM could involve increasing the number of production drifts per sublevel. In this experiment, each sublevel was limited to 2 or 3 production drifts. By augmenting the number of drifts per sublevel uniformly, a higher recovery rate could potentially be achieved. Additionally, the experiments utilized only 4 ore sublevels with a sublevel height of 10 m. Elevating the sublevel height and/or increasing the number of sublevels, such as raising the number to 5, could also lead to a further improvement in ore recovery rates.

The waste rock blending rate remains comparatively high in both COGDM and IDM due to the utilization of the cut-off grade method to stop loading at each drawing step and production drift within SLC. Particularly in IDM, where each drawing step involves the opening and closing of three directions of insert panels, resulting in three times of cut-off grade drawing, the waste rock mixing rate is notably elevated. Zhang and Liu proposed a 'non-dilution draw' method in which loading should be stopped as soon as dilution is encountered at the drawpoint. Physical modeling outcomes indicate a dilution range of 4–6% for the non-dilution draw method compared to 15–30% for the cut-off grade method, while maintaining consistent ore recovery objectives[34]. Hence, the non-dilution draw method could be implemented in IDM to further mitigate ore dilution.

Implementing insert structures in mining production drifts not only increases workload and production costs but also poses challenges in swiftly inserting or removing the insert plates during actual production. The use of steel plates as insert plates raises material considerations, as the choice between materials like transparent acrylic plates, wooden boards, or other materials can influence ore flow. Selecting the appropriate material for the insert structure is crucial to balancing cost reduction with maintaining adequate strength. Therefore, it is necessary to conduct a reasonable evaluation of economic performance of the insert drawing technique. If the economic benefits of mining more ores brought by this technique are much greater than the cost of IDM, it is possible to further promote and apply it in many other SLC mines. For successful field implementation of the proposed insert drawing technology, the critical factor lies in the effective insertion and extraction of insert plates. While

these operations are readily achievable in laboratory settings, field trials have not yet been conducted. Further research is required to facilitate the practical application of this technology in mining operations.

The relationships among the draw body, blasting body, and ore residual body in mining operations are intricate and interconnected. Presently, research on the blasting body is limited, often treating it as a regular shape. However, observations by some researchers suggest that the material blasted can move up to 1.2–1.6 m in the upper part of the drift due to the sudden release of a significant amount of detonation energy. This indicates that the ore-rock contact interface may not be as uniform as assumed in experiments[36,37]. Understanding the form of the ore residual body is also challenging. There is a lack of research on the formation pattern of the ore post-blasting, known as the blasting body, which is crucial for ore extraction. Further investigations are necessary on aspects such as ore fragmentation size distribution, loose coefficient, and fluidity within the blasting body. Field measurements or monitoring techniques like muography can help determine the shape and position of the blasting body and ore residual body, considering the differing densities of ore and rock[15]. To effectively manage ore loss and dilution in SLC method, it is essential to integrate blasting, drawing, and other processes as a cohesive unit for comprehensive study and control.

In the analysis of mechanisms to minimize ore loss and dilution using the IDM, the current approach has been qualitative and simplistic. Moving forward, it is recommended to incorporate advanced draw theories, such as random medium draw theory or expectation body theory, to quantitatively calculate the ore recovery rate and dilution rate during the drawing process with IDM. The quantitative calculation can be based on ellipsoid draw theory, random medium draw theory or expectation body theory. During the calculation of the drawing process, the amount of ore drawn, the amount of waste rock mixed in, and the amount of pure ore drawn can be calculated, so as to derive the theoretical calculation formulas for the recovery and dilution rate. By using the quantitative calculation method, as long as the relevant flow parameters of the blasted ore-rock are given, the ore recovery and dilution rate can be calculated, providing a method for predicting the loss and dilution of ore. This part of the research work is currently underway and will be publicly published soon. In addition, gravity flow and flow simulation techniques, such as REBOP or PCSLC software, may be used to predict flow behavior and material extracted at the drawpoint[38]. This approach can help in understanding how to control the movement of the waste rock funnel and the ore-rock contact from a theoretical perspective. Ongoing studies are focusing on these aspects, and the research results are expected to be published soon. By leveraging more sophisticated draw theories and analytical frameworks, researchers can gain deeper insights into optimizing ore recovery, reducing dilution, and enhancing the efficiency of the drawing process with IDM.

## Conclusions

In SLC mining, high ore loss and dilution are common issues, particularly in the extraction of steeply inclined medium-thick orebodies. Various factors influence ore loss and dilution in SLC mining, including geology, overburden rock, stope structure parameters, and ore-drawing management, etc. While some factors are interrelated or beyond human control, others, such as blasting, stope structure parameters, and draw management, are controllable.

The main types of ore residues in SLC mining include ridge remnants, frontal remnants, wall-adhering remnants, and foot-wall remnants. Residual ores can move towards the drawpoints under the influence of caved waste rocks, allowing for partial or complete extraction from the drawpoints. However, the confined flow conditions, chaotic and random nature of material flow in SLC, and the impact of blasting extrusion make it difficult to effectively control the contact and movement of blasted ores and caved waste rocks during extraction. The formation mechanism of waste rock funnel was analyzed. It is pointed out that the primary reason for ore dilution is the rupture of waste rock funnels from four directions near the drawpoint. Meanwhile, the mixing of ore and rock generated during the blasting process, as well as the mixing of ore and rock during the flow process, are also contributing factors to ore dilution.

The insert drawing technique, inspired by silo insert structures, has been introduced to mitigate ore loss and dilution in SLC mining. Furthermore, the mechanism of the insert drawing technique was analyzed. This technique involves actively controlling the contact, movement direction, and path of ore and rock near the drawpoints in the production drifts by adjusting the opening and closing of three-direction insert plates; Meanwhile, through the strategic adjustment of these insert plates, the technique effectively enhances ore flow speed and flow area, leading to improved ore recovery outcomes. By exerting control over the movement of the waste rock funnel, the technique can effectively delay rupture and the eventual arrival at the drawpoint, thereby curbing ore dilution.

Comparative experiments between the IDM and COGDM have shown that IDM yields a higher ore recovery rate than COGDM, with comparable waste rock blending rates. For massive orebodies, IDM can achieve a 10.96% higher ore recovery rate compared to COGDM. Moreover, for steeply inclined medium-thick orebodies, IDM can achieve a higher ore recovery rate ranging from 15.68 to 30.88%, accompanied by an average decrease of 3.95% in the waste rock blending rate when compared to COGDM.

Research demonstrates that the insert drawing method outperforms the conventional cut-off grade drawing method, effectively reducing ore residual and waste mixing in SLC mining through the insert drawing technique. This technique shows promise for wider adoption in other sublevel caving mines to improve ore recovery rates and operational efficiency. Recently, significantly propelled by advancements in drilling and blasting technologies, sublevel mining operations are now typically executed within vertical intervals spanning 20–35 m[39]. Concurrently, there is a discernible upward trajectory in the width of drawpoints, with dimensions expanding to 7–11 m in certain cases. This also provides a broader prospect for the application of insert drawing method.

## Data availability

## References

1. Janelid, I. & Kvapil, R. Sublevel caving. *Int. J. Rock Mech. Min. Sci.* **3**, 129–153 (1966).
2. Kvapil, R. The mechanics and design of sublevel caving systems. In *Underground Mining Methods Handbook* (ed. Hustrulid, W. A.) 880–897 (Society of Mining Engineers of the American Institute of Mining, Metallurgical, and Petroleum Engineers, 1982).
3. Hustrulid, W. & Kvapil, R. Sublevel caving—Past and future. *Newsl. Aust. Cent. Geomech.* **33**, 1–6 (2009).
4. Freidin, A. M. & Neverov, S. A. Modeling of area-end ore drawing under caved rocks. *J. Min. Sci.* **41**(5), 436–446 (2005).
5. Brunton, I. D., Fraser, S. J., Hodgkinson, J. H. & Stewart, P. C. Parameters influencing full scale sublevel caving material recovery at the Ridgeway gold mine. *Int. J. Rock Mech. Min. Sci.* **47**(4), 647–656 (2010).
6. Zhang, Z. X., Hou, D. F., Aladejarea, A., Ozojia, T. & Qiao, Y. World mineral loss and possibility to increase ore recovery ratio in mining production. *Int. J. Min. Reclam. Environ.* **35**(9), 670–691 (2021).
7. Shao, A. L. *Movement Rule of Waste Rock and Its Control Technology in Sublevel Caving Drawing* (Metallurgical Industry Press, 2013) (**in Chinese**).
8. Gustafsson, P. *Waste Rock Content Variations During Gravity Flow in Sublevel Caving: Analysis of Full-Scale Experiments and Numerical Simulations*. Dissertation, Luleå University of Technology, Luleå (1998).
9. Wimmer, M. *Gravity Flow of Broken Rock in Sublevel Caving (SLC)—State-of-the-Art*. Dissertation, Luleå University of Technology, Luleå (2010).
10. Liang, W. *The Mechanism of Wire Rope-Concrete-Flexible Artificial Roof in Ore-Drawing Under the Waste for Steeply Inclined Ore Body*. Dissertation, Kunming University of Science and Technology (2015) (**in Chinese**).
11. Malakhov, I'M. *Drawing of Caving Ore Block* (Metallurgical Industry Press, 1958) (**in Chinese**).
12. Chen, Q. F., Zhao, F. Y., Wang, Y. D. & Zhong, Y. Orthogonal simulation experiment for flow characteristics of ore in ore drawing and influencing factors in a single funnel under a flexible isolation layer. *JOM* **69**(12), 2485–2491 (2017).
13. Cao, J. L., Ren, F. Y., Zhang, J. J. & Yang, Q. P. Experimental study on diversion drawing by stress-relieve sublevel caving method. *J. Northeast. Univ. (Nat. Sci.)* **32**, 1186–1189 (2011) (**in Chinese**).
14. Tao, G. Q., Lu, M. X., Zhang, X. F., Zhang, R. & Zhu, Z. H. A new diversion drawing technique for controlling ore loss and dilution during longitudinal sublevel caving. *Int. J. Rock Mech. Min. Sci.* **113**, 163–171 (2019).
15. Zhang, Z. X. Lost-ore mining—A supplementary mining method to sublevel caving. *Int. J. Rock Mech. Min. Sci.* **168**, 105420 (2023).
16. Kvapil, R. Gravity flow of granular material in hoppers and bins. *Int. J. Rock Mech. Min. Sci.* **2**, 35–41 (1965).
17. Wang, C. H. *Draw Theory* (Metallurgical Industry Press, 1982) (**in Chinese**).
18. Rustan, A. Gravity flow of broken rock-What is known and unknown. In *Proceedings of MassMin. Brisbane; 29 October–2 November*, 557–568 (2000).
19. Litwiniszyn, J. Application of the equation of stochastic processes to mechanics of loose bodies. *Arch. Mech.* **8**(4), 393–411 (1956).
20. Ren, F. Y. *Stochastic Medium Theory for Draw and Its Application* (Metallurgical Industry Press, 1994) (**in Chinese**).
21. Chen, G. Stochastic modelling of rock fragment flow under gravity. *Int. J. Rock Mech. Min. Sci.* **34**(2), 323–331 (1997).
22. Jin, A. B., Sun, H., Wu, S. C. & Gao, Y. T. Confirmation of the upside-down drop shape theory in gravity flow and development of a new empirical equation to calculate the shape. *Int. J. Rock Mech. Min. Sci.* **92**, 91–98 (2017).
23. Sun, H. et al. A study of gravity flow based on the upside-down drop shape theory and considering rock shape and breakage. *Rock Mech. Rock Eng.* **52**(3), 881–893 (2018).
24. Sun, D. et al. Flow mechanisms and solid flow rate prediction of powders discharged from hoppers with an insert. *Powder Technol.* **367**, 277–284 (2020).
25. Cao, J. K. *Hopper Discharge of Fine Powders and Modeling Analysis*. Dissertation. East China University of Science and Technology, Shanghai, China (2021) (**in Chinese**).
26. Wojcik, M., Tejchman, J. & Enstad, G. G. Confined granular flow in silos with inserts-full-scale experiments. *Powder Technol.* **222**, 15–36 (2012).
27. Yang, S. C. & Hsiau, S. S. The simulation and experimental study of granular materials discharged from a silo with the placement of inserts. *Powder Technol.* **120**(3), 244–255 (2001).
28. Kobyłka, R., Molenda, M. & Horabik, J. Loads on grain silo insert discs, cones, and cylinders: Experiment and DEM analysis. *Powder Technol.* **343**, 521–532 (2019).
29. Tao, G. Q., Zhang, G., Wu, Y. X., Yin, G., Long, T. & Liang, B. An efficient mining method based on the insert action. Chinese patent. Hunan Province: CN113137232B. 2021-07-20 (**in Chinese**).
30. An, L. *Gravity Flow of Broken Rocks and the Control of Rock Blasting in Mining Narrow Steeply Dipping Veins*. Dissertation. Northeastern University, Liaoning, China (2015) (**in Chinese**).
31. Castro, R., Trueman, R. & Halim, A. A study of isolated draw zones in block caving mines by means of a large 3D physical model. *Int. J. Rock Mech. Min. Sci.* **44**(6), 860–870 (2007).
32. Trueman, R., Castro, R. & Halim, A. Study of multiple draw-zone interaction in block caving mines by means of a large 3D physical model. *Int. J. Rock Mech. Min. Sci.* **45**(7), 1044–1051 (2008).
33. Lapčević, V. & Torbica, S. Numerical investigation of caved rock mass friction and fragmentation change influence on gravity flow formation in sublevel caving. *Minerals* **7**(4), 56 (2017).
34. Liu, X. G. & Zhang, Z. G. Theory basis of ore-drawing without dilution for sublevel caving method (First part). *Met. Mine* **10**, 5–9 (1995) (**in Chinese**).
35. Wang, L. C., Jing, H. D., Yu, J. Y. & Liu, X. B. Impact of particle shape, size, and size distribution on gravity flow behaviour of broken ore in sublevel caving. *Minerals* **12**(10), 1183 (2022).
36. Wimmer, M., Nordqvist, A., Ouchterlony, F., Nyberg, U. & Furtney, J. K. Burden movement in confined drift wall blasting tests studied at the LKAB Kiruna SLC mine. In *Proceedings of the 10th International Symposium on Rock Fragmentation and by Blasting*, 373–383 (Taylor & Francis Group, London, 2013).
37. Power, G. Full scale SLC draw trials at ridgeway gold mine. In *Proceedings of the 4th International Conference and Exhibition on Mass Mining, Chile, Santiago*, 225–230 (2004).
38. Shekhar, G., Gustafson, A., Boeg-Jensen, P., Malmgren, L. & Schunnesson, H. Mathematical programming application in sublevel caving production scheduling. *J. S. Afr. I Min. Metall.* **118**, 723–733 (2018).
39. Khazaei, S. & Pourrahimian, Y. Mathematical programming application in sublevel caving production scheduling. *Mining* **1**, 180–191 (2021).

### Author contributions

G.T provided the original idea; X.M wrote the main manuscript text; X.M and T.L provided the data in this paper; X.S and L.W made the figures of this paper; Z.Z is responsible for review and editing.

### Funding

### Declarations

### Competing interests

The authors declare no competing interests.

### Additional information

**Correspondence** and requests for materials should be addressed to G.T.

**Reprints and permissions information** is available at www.nature.com/reprints.

**Publisher's note** Springer Nature remains neutral with regard to jurisdictional claims in published maps and institutional affiliations.